Biosensors and Bioelectronics 139 (2019) 111323

Contents lists available at ScienceDirect

Biosensors and Bioelectronics

journal homepage: www.elsevier.com/locate/bios

Amperometric glucose biosensing performance of a novel graphene nanoplatelets-iron phthalocyanine incorporated conducting hydrogel

H. Al-Sagur[a,b], Komathi Shanmuga sundaram[a,*], E.N. Kaya[c], M. Durmuş[c], T.V. Basova[d,e], A. Hassan[a]

[a] Materials and Engineering Research Institute, Sheffield Hallam University, Sheffield, UK
[b] Department of Physiology and Medical Physics, College of Medicine, University of Thi-Qar, Nasiriyah, Iraq
[c] Gebze Technical University, Department of Chemistry, Gebze, 41400, Kocaeli, Turkey
[d] Nikolaev Institutes of Inorganic Chemistry SB RAS, Lavrentiev Pr. 3, Novosibirsk, 630090, Russia
[e] Novosibirsk State University, Pirogova Str. 2, Russia

ARTICLE INFO

Keywords:
Conducting hydrogel
Water-soluble iron phthalocyanine
Glucose biosensor
Graphene nanoplatelets (GPL)

ABSTRACT

Herein, a novel one step synthesis of multicomponent three dimensional polyacrylic acid (PAA) based conducting hydrogel (CH) incorporated with iron phthalocyanine functionalised graphene nanoplatelets (GPL-FePc) is reported. An amperometric glucose biosensor was fabricated by the immobilization of glucose oxidase (GOx) onto the synthesised PAA-VS-PANI/GPL-FePc-CH (where VS-PANI is vinyl substituted polyaniline). Scanning electron microscopy reveals the presence of three dimensional microporous structure with estimated pore size of 19 μm. The 5-(trifluoromethyl)-2-mercaptopyridine substitution onto FePc enabled the solubility of FePc in water and controls the aggregation of GPL-FePc in the synthesised CH. A sharp peak around 699 nm in UV–visible spectra confirms the presence of incorporated GPL-FePc into CH. Cyclic voltammogram of the synthesised CH biosensor exhibited well defined redox peaks with a ΔE_p value of 0.26 V in $Fe(CN)_6^{3-/4-}$ bench mark solution. The fabricated PAA-VS-PANI/GPL-FePc/GO_x-CH amperometric biosensor resulted in remarkable detection sensitivity of 18.11 μA mM^{-1} cm^{-2} with an average response time of ~1 s, linearity from 1 to 20 mM, and low detection limit of 6.4 μM for the determination of glucose.

1. Introduction

Graphene is a single-atom-thick sheet of sp^2 hybridised carbon atoms which has received great attention in recent years due to its unique physical properties such as exceptional electrical conductivity, large specific surface area, and strong mechanical strength (Allen et al., 2010; Zhu et al., 2010). This makes graphene based composites a suitable candidate for biomolecules detection (Liu et al., 2016). Glucose oxidase (GOx) is the most widely used enzyme for amperometric glucose detection (Claussen et al., 2012). Unnikrishnan and co-workers reported electrochemical approach for the immobilization of glucose oxidase (GOx) onto reduced graphene oxide (RGO) electrode [Unnikrishnan et al., 2013 Biosensors and Bioelectronics Volume 39, Issue 1, 15 January 2013, Pages 70–75]. One of the major challenges in graphene based electrochemical biosensor construction is their uniform dispersion, where a single graphene layer tends to curl during dispersion for efficient electrocatalysis (Bo et al., 2017). Further, in the development of new biosensors, along with sensitivity, selectivity, and rapid detection, cost reduction are also taken into paramount considerations (Lawal, 2018; Novoselov et al., 2012). Hence in recent years, alternative embodiments of graphene nanostructures (e.g. platelets, sheets and ribbons) have been proposed (Akinbulu and Nyokong, 2010; Buber et al., 2017; Jan et al., 2017). Graphene nanoplatelets (GPL) are multi-layer particles consisting of 10–30 sheets of graphene and can be produced relatively inexpensively (Jan et al., 2017). It is demonstrated that GPLs possess high chemical stability, biocompatibility and large effective surface area that are advantageous for the construction of electrochemical biosensors (Gong et al., 2012; Li et al., 2016; Lawal, 2018; Schedin et al., 2007).

On the other hand, metallophthalocyanines (MPcs) (e.g., CoPc, CuPc, FePc and NiPc) are a versatile class of organic compounds known to exhibit good electrocatalysis towards the oxidation of biological compounds (Agboola et al., 2009; Chaiyo et al., 2018; Foster et al., 2014). MPcs have also been used as redox mediators in biosensors construction (Al-Sagur et al., 2018; Devasenathipathy et al., 2015; Özcan et al., 2008). Perhaps the insolubility of MPcs in water and

* Corresponding author.
E-mail addresses: skomu83@gmail.com, K.shanmugasundaram@shu.ac.uk (K. Shanmuga sundaram).

https://doi.org/10.1016/j.bios.2019.111323
Received 11 March 2019; Received in revised form 3 May 2019; Accepted 12 May 2019
Available online 16 May 2019
0956-5663/

common organic solvents limits their wide application in biosensor devices. Henceforth many water-soluble Pcs have been synthesised by introducing hydrophilic moieties, such as carboxylate, sulfonate, phosphonate, polyoxyethylene, amino and carboxyl groups (Baygu and Gök, 2018; Muckley et al., 2017). Zagal and co-workers in 1980 proposed the sulphate group modification that significantly improved solubility of MPcs in water and in organic solvents (Zagal et al., 1980). Water-soluble FePc have been applied in the catalytic oxidation of phenols (Gong et al., 2014), while water-soluble CoPc was shown to mediate and increase the signal response of an amperometric glucose biosensor (Fogel et al., 2007; Mashazi et al., 2006). However, water-soluble MPcs exhibited tendency to aggregate in solution (Iliev and Ileva, 1995; Kuznetsova et al., 2003). Recently, graphene modification with MPcs has received immense interest due to their unique combinational properties (Hosseini et al., 2014); these include redox properties, fast electron transfer kinetics, electrical conductivity, biocompatibility, high chemical and thermal stabilities which attribute the application of graphene nanostructures supported MPcs in glucose biosensors (Mani et al., 2014; Zhang et al., 2013).

Some of the recently reported biosensors that utilize graphene nanostructures supported MPcs for GOx immobilization include GR-CoPc/GOx (Mani et al., 2014), PAA-rGO/VS-PANI/LuPc$_2$/GOx-MFH (Al-Sagur et al., 2017), CoPc/IL/G (Chaiyo et al., 2018), nanoCoPc-Gr/GOx (Wang et al., 2015), GR-CoPc and GR-FePc (Mani et al., 2015), and GOD/Nafion/(LbL)3.5/ABS/GCE (Zhang et al., 2013). Although there are few GR-MPcs/GOx-based glucose sensors reported, there are still remains challenges in the construction of efficient biosensors (Costa de Oliveira et al., 2017). Some of the limitations in the fabrication of GOx based biosensors are (i) amount of enzyme immobilization, (ii) electrical contact between the enzyme and basal electrode, (iii) enzyme leaching, (iv) biological activity and (v) shelf life. In order to overcome these limitations construction of a multicomponent and robust 3D matrix for the immobilization of enzyme would be an alternative approach. Hydrogels offer 3D cross-linked network structures of hydrophilic polymer chains (Ahmed, 2015). Hydrogel networks formed from polyacrylic acid (PAA) are classified as super absorbents and have the ability to absorb water more than its weight (Dhodapkar et al., 2009). PAA hydrogel plays an important role as pH stimuli-responsive and bioadhesive material because of the presence of –COOH groups in their chain (Arunbabu et al., 2013). The incorporation of nanomaterials such as graphene within the 3D network either physically or covalently embrace various functionalities to hydrogels (Goenka et al., 2014). Reports are also available on the use of a hydrogel consisting of ferrocene or osmium complex to wire GOx to the electrode surface (Calvo et al., 1993; Gregg and Heller, 1991). The introduction of a conducting polymer such as polyaniline (PANI) onto the hydrogel would potentially impart electrical communication between the immobilised enzyme to the electrode surface. Beside electronic conductivity, PANI lined within the hydrogel contributes ionic conductivity in aqueous media, electrochemical reversibility, good flexibility and mechanical integrity. Nontoxicity and compatibility, porosity and high specific surface area, macroscopic homogeneity and controlled morphology are among other unique properties of PANI (Malti et al., 2016; Shahid et al., 2018).

From infancy up to old age diabetes mellitus (DM) dramatically affect life of men and women (International Diabetes Federation, 2017). DM is a significant reason for loss of vision, renal impairments, macrovascular complications, and lower limb amputations (WHO, 2016). Both biological – genetic and endocrine – as well as psychosocial and environmental factors are responsible for outcomes of diabetes (Kautzky-Willer et al., 2016). A sudden elevation in blood glucose causes glucose toxicity, leading to morbidity and mortality among diabetic patients (Poitout et al., 2006). Therefore, there is an increasing demand for the development of fast and reliable platforms for the detection of glucose. In addition, detection of glucose is also widely essential in food industries to monitor the quality of the products along the production and supply chain (Guadarrama-Fernández et al., 2018). Electrochemical sensors have been widely used for point of care detection of glucose in recent decades for its unique sensing performance such as fast response and high sensitivity (Gosselin et al., 2017; Pu et al., 2017). The electrochemical meters are simple in fabrication, convenient for operation and easy in transportation. Therefore electrochemical sensors are broadly applied in the biological, food and clinical fields (Bahadir and Sezgintürk, 2015; Lv et al., 2018).

Although sufficient work has been carried out using GR-MPcs as mediators in sensor studies, the use of water processable GPL-FePc into conducting hydrogel (CH) platform has not yet been reported. Herein, a new multicomponent based robust 3D matrix for the immobilization of GOx is reported. The multicomponent conducting hydrogel (CH) include polyacrylic acid (PAA), vinyl substituted polyaniline (VS-PANI), water-soluble FePc functionalised GPL (PAA-VS-PANI/GPL-FePc/GOx-CH). The cationic quaternized 5-(trifluoromethyl)-2-N-methylmercaptopyridine substituents in FePc molecule provide its strong non-covalent bonding with GPL and high dispersibility in the formed hydrogel. The integration of PAA with GPL-FePc and VS-PANI were all carried out in one step through free radical polymerization using methylene bisacrylamide as the cross linker and initiator. Finally, the biosensor was fabricated by immobilising GOx into PAA-VS-PANI/GPL-FePc/GOx-CH and subsequently used for electrochemical detection of glucose.

2. Experimental details

2.1. Materials

Graphene nanoplatelets (GPL) has a surface area: 500 m^2/g, surfactant type: anionic surfactant, sheet resistance: 10 (± 5) Ω/sq (for a 25 μm film), and the sheet has been packed at around 5–7 atomic layers), poly(ethylene glycol) diamine (NH_2-PEG-NH_2), N-(3-dimethylaminopropyl)-N′-ethylcarbodiimide hydrochloride (EDC hydrochloride), acrylic acid, 3-vinylaniline (97%), N,N′-methylenebis(acrylamide) (MBA), ammonium persulfate (APS), D-(+)glucose, glucose oxidase from Aspergillus niger (Type X–S, lyophilised powder, 100,000–250,000 units/g solid, without added oxygen), glutaraldehyde solution (Grade II, 25% in H_2O), potassium ferrocyanide, potassium ferricyanide, potassium chloride (KCl), sodium chloride (NaCl), phosphate buffer solution (PBS, pH 7.0), hydrochloric acid (HCl, 37% solution in water), ascorbic acid, uric acid and human serum were purchased from Sigma Aldrich (UK) and used as received. Water soluble cationic quaternized 5-(trifluoromethyl)-2-N-methylmercaptopyridine substituted FePc was synthesised from 4,5-dichlorophthalonitrile and purified according to the reported procedure. The detailed synthesis of water soluble FePc and its characterisations are presented in supporting information (SI-1). All the reaction solvents were of reagent grade and purified as received.

2.2. Instruments

The morphologies of the as prepared PAA-VS-PANI/GPL-FePc-CH were examined by FEI-Nova scanning electron microscopy (SEM) with a low magnification (160,000 ×) and high voltage (10 kV). UV–visible spectrophotometer (Varian 50-scan UV–visible) in the range 190–1100 nm was used to measure the absorption spectra of the hydrogel. FT-IR spectra were recorded on a PerkinElmer Spectrum 100 spectrophotometer. The electrochemical measurements of the modified electrodes were conducted using a portable multi Potentiostat/Galvanostat μStat 8000 and controlled by PC with DropView 8400 software by DropSens (Spain). The sensor platforms were fabricated on disposable screen-printed carbon electrodes (DRP-C110) with 4 mm diameter working electrode. The working and auxiliary electrodes are carbon, while silver forms the reference electrode and the träger (carrier) is ceramic. The working electrodes were modified with PAA-VS-PANI/GPL-FePc/GOx-CH or PAA-VS-PANI/GPL-FePc-CH or PAA-VS-

PANI/GPL-GOx-CH. The electroactivity of biosensors were evaluated by recording cyclic voltammogram in potassium ferro/ferricyanide solution containing 0.1 M NaCl in the potential range from −0.5 V to +0.5 V. The amperometric responses of PAA-VS-PANI/GPL-FePc/GOx-CH biosensor towards glucose detection were recorded under stirred conditions in 0.1 M PBS (pH 7.0) by applying a constant potential of +0.3 V at the working electrode.

2.3. Preparation of PAA-VS-PANI/GPL-FePc/GOx-CH biosensor

The preparation of PAA-VS-PANI/GPL-FePc/GOx-CH involves three steps: (1) synthesis of water-soluble FePc functionalised GPL (GPL-FePc), (2) formation of PAA-VS-PANI/GPL-FePc-CH, and (3) immobilization of GOx.

2.3.1. Preparation of water soluble FePc non-covalently functionalised GPL (GPL-FePc)

About 1 mg of the synthesised FePc (SI-1(ii)) was dissolved in 10 mL of deionised water under magnetic stirring (500 rpm). To this FePc solution, 10 mg of GPL was added and ultra-sonicated for about 30 min. GPL non-covalently functionalised with FePc (GPL-FePc) were then filtered through polycarbonate membrane (pore size = 200 nm) and dried at 60 °C for about 24 h (till constant weight is obtained) under vacuum condition. 10 mg of GPL-FePc thus obtained was dispersed in 10 mL of deionised water under sonication. To this NH_2-PEG-NH_2 (0.1 g) and EDC.HCl (0.1 g) were added under vigorous stirring overnight. The amine functionalised GPL-FePc thus obtained was then filtered and dried as before in vacuum oven at 60 °C for further use. The dispersion stability of the synthesised amine functionalised GPL-FePc was verified by stand by analysis. 1 mg of the sample was dispersed in 10 mL of deionised water under sonication for 30 min. The bottle was allowed to stand untouched for about a week, when a uniform dispersion of GPL-FePc in the medium was obtained with no settling for nearly 5 days. The ^{1}H-NMR spectrum of 4,5-bis[5-(trifluoromethyl)-2-mercaptopyridine]phthalonitrile (**1**) has been studied in order to prove the molecular structure of the composite (SI-1).

2.3.2. Formation of PAA-VS-PANI/GPL-FePc-CH

5 mg of amine functionalised GPL-FePc was dispersed in 10 mL of HCl (0.1 M) containing 10 mg of EDC.HCl under sonication. Subsequently, AA (2.4 mL), MBA (2 M), 3-vinylaniline (0.1 M) and APS (0.2 M) were added into the mixture with continued stirring. The above solution mixture was purged with N_2 gas to remove the dissolved oxygen content and poured into a pre-cleaned vial. The vial was placed in vacuum oven maintained at 70 °C for about an hour. A solid hydrogel was formed after about 40 min. After the gelation is completed, the solid was cooled to room temperature. The colour of the solid hydrogel turned to light green with uniformly distributed black tints to form PAA-VS-PANI/GPL-FePc-CH (Scheme 1). For comparative purposes, hydrogels have also been formed through the exclusion or inclusion of FePc and 3-vinylaniline or without both; the so formed hydrogels are PAA-VS-PANI/GPL-CH, PAA/GPL-FePc-CH, and PAA/GPL-CH, respectively. We noticed diversity in the gelation time of individual hydrogel, i.e., PAA-VS-PANI/GPL-CH (~45 min), PAA/GPL-FePc-CH (~75 min), PAA/GPL-CH (~85 min) respectively.

2.3.3. Fabrication of PAA-VS-PANI/GPL-FePc/GOx-CH biosensor

Initially PAA-VS-PANI/GPL-FePc-CH (2 µl) was formed on the surface of screen-printed carbon electrode (Area = 0.1256 cm^2), and allowed to dry in oven at 70 °C. The fabrication of PAA-VS-PANI/GPL-FePc/GOx-CH biosensor electrode was carried out by immobilising GO_x (1 µl) (10 mg in 1 mL PBS (pH 7.0)) along with glutaraldehyde (1 µl) as cross-linker and dried at room temperature for further use. Similarly, PAA-VS-PANI/GPL/GOx-CH, PAA/GPL-FePc/GOx-CH, and PAA/GPL/GOx-CH biosensor electrodes were fabricated for comparative purpose.

3. Results and discussions

3.1. Formation of PAA-VS-PANI/GPL-FePc-CH

The formation of *PAA-VS-PANI/GPL-FePc-CH* is presented in Scheme 1. PAA-VS-PANI/GPL-FePc-CH was formed through free radical polymerization of AA along with amine functionalised GPL-FePc and 3-vinylaniline in the presence of MBA and APS (Layek and Nandi, 2013). We carried out the polymerization as reported in our earlier work (Al-Sagur et al., 2017). Herein, we presume the inclusions of water processable GPL-FePc in the hydrogel provides additional binding sites for the immobilization of GOx along with the beneficiaries of PAA and VS-PANI. PAA results in robust 3D assembly and –COOH groups protect VS-PANI in its protonated form. Scheme 1 shows the photograph of *PAA-VS-PANI/GPL-FePc-CH* before *(vertical vial)* and after hydrogel formation *(inverted vial)*. The hydrogel exhibits green colour of protonated VS-PANI with well dispersed black tints of GPL-FePc. The swelling ratio of the sensing platform has been studied in order to examine the impact of the various components of the conducting hydrogel (see SI-2).

3.2. Morphology

The SEM image of PAA-VS-PANI/GPL-FePc-CH (Scheme 1 and in SI-3(a)) shows clear micro porous 3D structure. The 3D structure resulted from the precise self assembly of the individual components to form an interconnected network within the hydrogel. The pore size of the formed PAA-VS-PANI/GPL-FePc-CH was estimated to be 19 µm (calculated from SEM analysis). The pore size of PAA- VS-PANI/GPL-FePc-CH was adequate for excess loading of GOx and mass transport of analyte during analysis. The SEM image of PAA-VS-PANI/FePc-CH (formed in the absence of GPL) is presented in SI-3(b). It shows smooth surface with much small pore size compared to PAA-VS-PANI/GPL-FePc-CH. This illustrates the role of GPL in the hydrogel matrix in the self-assembly of the monomer and the cross-linker to form the conducting polymer (Chirani et al., 2015).

3.3. UV–visible absorption spectra

UV–visible absorption spectra of FePc and the other conducting hydrogels including PAA-VS-PANI/GPL-FePc-CH have been studied and results are given in SI-4 and Fig. 1, respectively. The UV–visible spectrum of PAA-VS-PANI/GPL-FePc-CH and PAA-VS-PANI/GPL-CH shows the corresponding band absorptions of PANI π–π* transition of benzenoid ring around 440 nm and n–π* transition of benzenoid to quinoid around 620 nm respectively (Fig. 1) (Chaiyo et al., 2018; Muckley et al., 2017). However, PAA-VS-PANI/GPL-FePc-CH shows an additional sharp peak around 699 nm corresponding to FePc in addition to absorption peaks of PANI. This indicates that GPL-FePc are well dispersed within the hydrogel. Furthermore, the molecular structure of the hydrogels prepared was inferred by recording FTIR spectra in absorption mode and the results were presented in SI-5.

3.4. Electrochemical performance of modified electrodes

Cyclic voltammograms (CVs) of (i) bare electrode, (ii) pristine GPL and (iii) water soluble FePc modified electrodes were recorded in 5 mM of $Fe(CN)_6^{3-/4-}$ solution containing 0.1 M NaCl (Fig. 2A). An identical redox couple corresponding to Fe(II)/Fe(III) could be seen at bare (Fig. 2A(a)) (0.26 V(Epa)/-0.03 V(Epc)) and pristine GPL (b) (0.25 V (Epa)/0.03 V(Epc)) (Fig. 2A(b)) modified electrodes. A difference in background current is explained by a different conditions of the electrode (modified–unmodified). Although the presence of GPL increased the electron transfer rate (ΔEp = 0.22 V) and catalytic current (~1.52 times), it does not alter the shape of the reversible system. In the case of water soluble FePc modified electrode four oxidation and two reduction

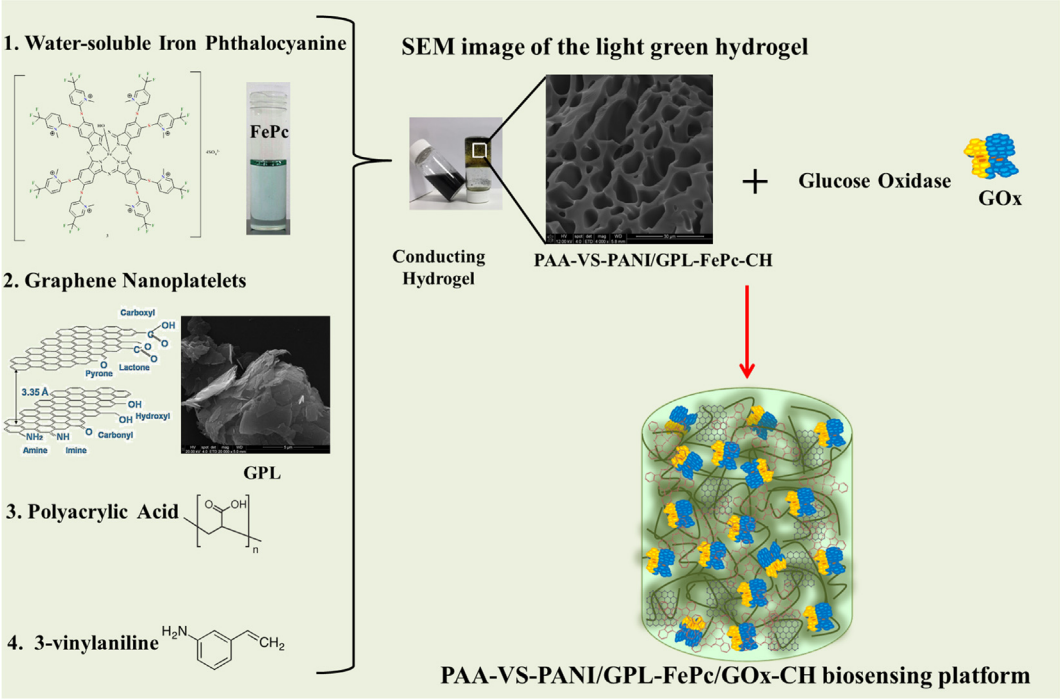

Scheme 1. Procedure of formation of PAA-VS-PANI/GPL-FePc/GOx-CH.

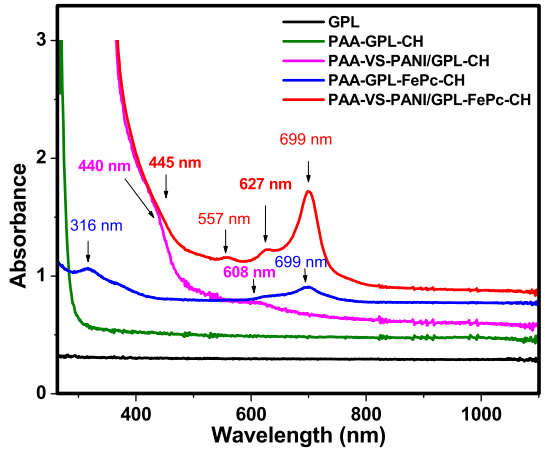

Fig. 1. UV–visible spectra of hydrogel modified electrodes.

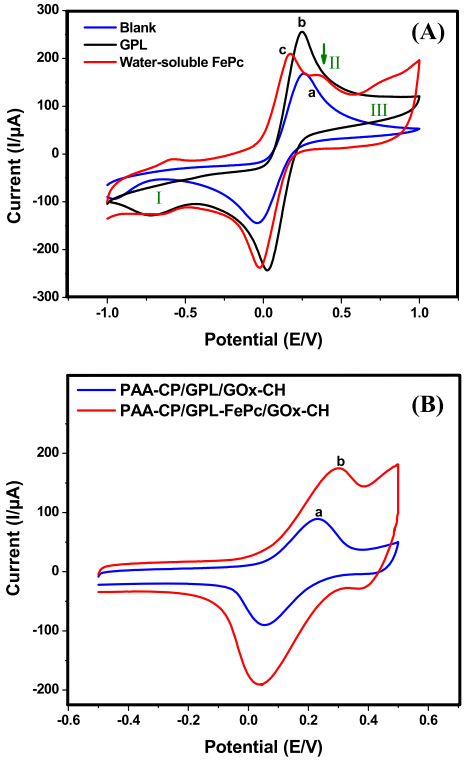

Fig. 2. CVs: (A) – pristine SPCE (a), GPL (b), FePc (c); (B) – PAA-VS-PANI/GPL/GOx-CH (a), PAA-VS-PANI/GPL-FePc/GOx-CH (c), recorded in 5 mM of $Fe(CN)_6^{-3/-4}$ solution containing 0.1 M NaCl as a supporting electrolyte versus Ag/AgCl at scan rate = 100 mV/s.

peaks were observed (Fig. 2A(c)). Oxidation peaks (I), (II) and (III) (Fig. 2A(c)) are assigned to charge transfer process occurring on the ligand without the involvement of the Fe centre as Fe(II)Pc/Fe(II)Pc^{-1} (Alsudairi et al., 2017), Fe(I)Pc/Fe(II)Pc and Fe(II)Pc/Fe(III)Pc respectively. While peak (I) is electrochemically and chemically reversible with respect to ΔEp and Ipa/Ipc values, peak (II) and peak (III) have chemically quasi-reversible character. The central metal ions having higher oxidation state have coordination tendency with the coordinating agent in the electrolyte (Demirbaş et al., 2016; Leznoff and Lever, 1996).

CV was also recorded for GOx immobilised hydrogel biosensor (i) PAA-VS-PANI/GPL/GOx-CH (curve a), (ii) PAA-VS-PANI/GPL-FePc/GOx-CH (curve b) in the potential range from −0.5 to +0.5 V (Fig. 2B). ΔE_p value of PAA-VS-PANI/GPL-FePc/GO_x-CH (0.26 V) (Fig. 2B(b)) was slightly higher than PAA-VS-PANI/GPL/GO_x-CH biosensor (0.18 V) (Fig. 2B(a)). The Fe(II)/Fe(III) redox peak current at PAA-VS-PANI/GPL-FePc/GO_x-CH (Fig. 2B(b)) was ~2 times higher compared to PAA-VS-PANI/GPL/GO_x-CH based biosensor (Fig. 2B(a)). The higher electrocatalytic current ensures the increased redox reaction at PAA-VS-PANI/GPL-FePc/GO_x-CH biosensor (Fig. 2B(b)) possibly due the preferred orientation of GOx onto the FePc sites onto the hydrogel (Muckley et al., 2017; Zagal et al., 1980). Further, the stability of GOx at PAA-VS-PANI/GPL-FePc-CH biosensor was investigated by recording continuous CVs (50 times) at scan rate of 100 mV/s (SI-6). It could be

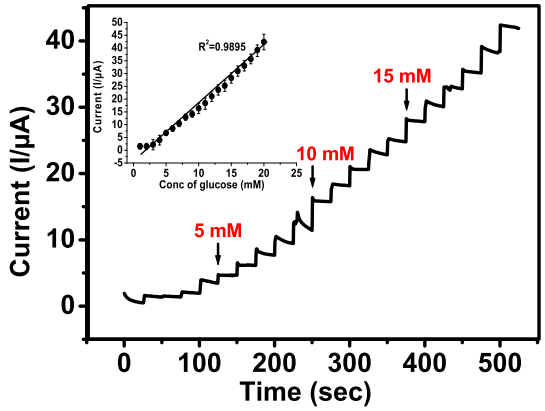

Fig. 3. Amperometric response of PAA-VA-PANI/GPL-FePc/GOx-CH to the addition of glucose
(1–
20
mM) in 0.1 M
PBS (pH 7.0). Inset: a calibration plot of peak current versus glucose concentration.

seen that CVs showed similar pattern even at the end of 50 cycles with negligible shift in ΔEp value. This confirms the robust 3D structure of PAA-VS-PANI/GPL-FePc-CH which provides an ideal platform for stable immobilization of GOx and substantially reduces leaching of enzyme onto the electrolyte during the course of reaction. CVs of PAA-VS-PANI/GPL-FePc/GO_x-CH biosensor were recorded for different scan rates (10–100 mV/s) (SI-7). The Ipa/Ipc increases with scan rate with a small shift in ΔEp value confirming a diffusion-controlled process. To support this inference, further electrochemical impedance spectroscopy (EIS) was recorded and presented in SI-8.

3.5. Amperometric response of PAA-VS-PANI/GPL-FePc/GO_x-CH biosensor

Amperometric current response for the oxidation of glucose at PAA-VS-PANI/GPL-FePc/GO_x-CH biosensor was measured under optimised conditions (potential = +0.3 V; 0.1 M PBS pH = 7.0) and the results are presented in Fig. 3. Linear current response was achieved for the glucose in the concentration range 1–20 mM with the correlation coefficient R of 0.985 as shown in the inset of Fig. 3. The plausible mechanism for the oxidation of glucose at PAA-VS-PANI/GPL-FePc/GOx-CH biosensor is as follows

$$GOx(FAD) + glucose + O_2 \rightarrow GOx(FADH_2) + glucanolactone + H_2O_2 \quad (1)$$

$$2[GPL\text{-}Fe(III)Pc] + GOx(FADH2) + H2O2 \rightarrow 2[GPL\text{-}Fe(II)Pc] + GOx(FAD) + O2 + 2H+ \quad (2)$$

$$2[GPL\text{-}Fe(II)Pc] + 2H+ \rightarrow 2[GPL\text{-}Fe(III)Pc] + 2e\text{-} \quad (3)$$

With the addition of glucose a large increase in amperometric current at PAA-VS-PANI/GPL-FePc/GOx-CH biosensor, under optimised conditions was observed. The increase in amperometric current with the successive addition of glucose was explained as follows; The added glucose is transferred from bulk solution to the biosensor through diffusion. GOx(FAD) converts glucose to gluconolactone and H_2O_2 through enzyme catalyzed reaction in the presence of natural co-substrate O_2. GPL-FePc bound within PAA-VS-PANI/GPL-FePc/GOx-CH which exist in (III) oxidation state oxidises the reduced form of GOx ($FADH_2$). The reduced GPL-Fe(II)Pc will be regenerated to its original form GPL-Fe(III)Pc under the applied potential of +0.3 V resulting in high amperometric current. This suggests that FePc mediates electron transfer between the immobilised GOx and the electrode through oxidation of the reduced form of the enzyme. A similar mechanism was reported for mediator based glucose oxidation by GOx immobilised electrodes (Ozoemena and Nyokong, 2006; Al-Sagur et al., 2017).

The sensor is shown to exhibit sensitivity of 18.11 μA mM^{-1} cm^{-2}; the limit of detection (LOD) of the biosensor was calculated to be 6.4 μM (S/N = 3) (Yang et al., 2004). The PAA-VS-PANI/GPL-FePc/GOx-CH biosensor showed rapid response to glucose with response time of ~1 s which is much less than recently reported glucose biosensors (Sode et al., 2017; Ullah et al., 2018). A comparison table showing the performance of the biosensor is presented in Table 1. SI-10 shows the performance of the PAA-VS-PANI/GPL-FePc/GOx-CH biosensor for ten repetitive measurements of glucose, reproducibility and the stability of biosensor.

3.6. Specificity and interference

The selectivity of PAA-VS-PANI/GPL-FePc/GOx–CH–based glucose biosensor has been also investigated by examining the biosensor on exposure to whole blood with interfering substances such as ascorbic acid and uric acid. Amperometric response current to 4 mM glucose (under optimised conditions) hardly affected by other interfering blood components such as AA and UA (SI-11(A))

3.7. Determination of glucose in real samples

To demonstrate the feasibility of PAA-VS-PANI/GPL-FePc/GOx-CH as viable biosensor for industrial applications, the detection of glucose in real samples (fruit juice and human serum) was performed. The continuous amperometry scans were recorded in different solutions under identical experimental conditions. PAA-VS-PANI/GPL-FePc/GO_x-CH biosensor exhibited response to all investigated real samples and the results are shown in SI-11(B) and summarised in the Table given in SI-12 (a). A satisfactory performance is clearly shown with an error margin of 3.8%, which demonstrates the viability of PAA-VS-PANI/GPL-FePc/GO_x-CH biosensor for glucose detection in real time application. Real sample analysis was also performed under diluted real samples and added into glucose solution. The results are presented in Tables SI–12 (b). Further importance of GOx and GPL-FePc in the fabricated biosensor was evaluated through amperometric

Table 1
Comparison of analytical performance of some glucose biosensor.

Electrode	Linear range (mM)	Sensitivity (μA. mM^{-1} cm^{-2})	Response time (s)	LOD (μM)	Ref
SPCE/CoPC/GOD	0.2–5	1.12	60	–	Crouch et al. (2005)
GCE–CoPc–$(CoTPP)_4$–GOx	Upto 11	0.024	~5	10	Ozoemena and Nyokong (2006)
PAA-rGO/VS-PANI/$LuPc_2$/GOx-MFH	2–12	15.31	~1	25	Al-Sagur et al. (2017)
Nafion/GOD@TiO2/FePc-CNT	0.05–4	7.71	12	30	Cui et al. (2013)
GR-CoPc/GOx	0.01–14.8	5.09		1.6	Mani et al. (2014)
PFLA/MWCNT/ZnPc/GOx	0.025–1	82.18		0.018	Buber et al. (2017)
Au-MPS-OsPVP-GOx	0.1–10		5	50	Hou et al. (1998)
{GOx/Au-(SH)PANI-g-MWNT}*n*/ITO	1–9	3.97	8	0.06	Komathi et al. (2009)
PAA-VS-PANI/GPL-FePc/GOx-CH	1–20	18.11	~1	6.4	This work

measurements and the results are presented and discussed in SI-12 (c).

4. Conclusion

In summary we have demonstrated the successful preparation of a simple one step novel three dimensional polyacrylic acid (PAA) based conducting hydrogel (CH) incorporated with vinyl substituted polyaniline (VS-PANI) and iron phthalocyanine functionalised graphene nanoplatelets (GPL-FePc) (PAA-VS-PANI/GPL-FePc-CH). An amperometric biosensor was fabricated with the immobilization of glucose oxidase onto the synthesised conducting hydrogel. The three dimensional microporous structure of PAA-VS-PANI/GPL-FePc-CH (19 μm) provided large surface area for the greater immobilization of enzyme. The water soluble nature of the synthesised 5-(trifluoromethyl)-2-N-methylmercaptopyridine substituted FePc limits the use of other organic solvents into the conducting hydrogel network and thus provided a biocompatible environment for the immobilised GOx. The water dispersible ability of GPL-FePc contributes for uniform dispersion of mediator within the conducting hydrogel. Cyclic voltammogram of PAA-VS-PANI/GPL-FePc-CH/GOx biosensor showed excellent electrocatalytic property with a ΔE_p value of 0.26 V in $Fe(CN)_6^{3-/4-}$ solution. The bio-electrocatalytic activity of the fabricated PAA-VS-PANI/GPL-FePc/GO_x-CH amperometric biosensor resulted in remarkable sensitivity of 18.11 $\mu A\, mM^{-1}\, cm^{-2}$ and showed wide linear range from 1 to 20 mM of glucose detection. We presume that the proposed three dimensional PAA based conducting hydrogel incorporated with GPL-FePc would remain as a promising platform for the fabrication of other enzyme based biosensors and bioelectronic devices in the near future.

CRediT authorship contribution statement

H. Al-Sagur: Formal analysis, Validation, Writing - original draft. **Komathi Shanmuga sundaram:** Conceptualization, Methodology, Writing - original draft, Writing - review & editing. **E.N. Kaya:** Formal analysis, Validation. **M. Durmuş:** Resources, Supervision. **T.V. Basova:** Resources, Supervision. **A. Hassan:** Supervision, Conceptualization, Writing - review & editing.

Acknowledgements

Hadi Al-Sagur acknowledges the financial support provided for his research from the Ministry of Higher Education and Scientific Research (MOHESR) and the College of Medicine/Thi Qar University southern of Iraq. T. Basova acknowledges FASO of Russian Federation for a financial support (project 0300-2016-0007).

Appendix A. Supplementary data

Supplementary data to this article can be found online at https://doi.org/10.1016/j.bios.2019.111323.

References

Agboola, B.O., Vilakazi, S.L., Ozoemena, K.I., 2009. Electrochemistry at cobalt(II)tetrasulfophthalocyanine-multi-walled carbon nanotubes modified glassy carbon electrode: a sensing platform for efficient suppression of ascorbic acid in the presence of epinephrine. J. Solid State Electrochem. 13, 1367–1379. https://doi.org/10.1007/s10008-008-0691-3.

Ahmed, E.M., 2015. Hydrogel: preparation, characterization, and applications: a review. J. Adv. Res. 6, 105–121. https://doi.org/10.1016/j.jare.2013.07.006.

Akinbulu, A.I., Nyokong, T., 2010. Fabrication and characterization of single walled carbon nanotubes-iron phthalocyanine nano-composite: surface properties and electron transport dynamics of its self assembled monolayer film. New J. Chem. 34, 2875. https://doi.org/10.1039/c0nj00395f.

Al-Sagur, H., Komathi, S., Karakaş, H., Atilla, D., Gürek, A.G., Basova, T., Farmilo, N., Hassan, A.K., 2018. A glucose biosensor based on novel Lutetium bis-phthalocyanine incorporated silica-polyaniline conducting nanobeads. Biosens. Bioelectron. 102, 637–645. https://doi.org/10.1016/j.bios.2017.12.004.

Al-Sagur, H., Komathi, S., Khan, M.A., Gurek, A.G., Hassan, A., 2017. A novel glucose sensor using lutetium phthalocyanine as redox mediator in reduced graphene oxide conducting polymer multifunctional hydrogel. Biosens. Bioelectron. 92, 638–645. https://doi.org/10.1016/j.bios.2016.10.038.

Allen, M., Tung, V., Kaner, R., 2010. Honeycomb carbon: a review of graphene. Chem. Rev. 110 (1), 132–145.

Alsudairi, A., Li, J., Ramaswamy, N., Mukerjee, S., Abraham, K.M., Jia, Q., 2017. Resolving the iron phthalocyanine redox transitions for ORR catalysis in aqueous media. J. Phys. Chem. Lett. 8, 2881–2886. https://doi.org/10.1021/acs.jpclett.7b01126.

Arunbabu, D., Shahsavan, H., Zhang, W., Zhao, B., 2013. Poly (AAc - co - MBA) hydrogel Films . adhesive and mechanical properties in aqueous medium. https://doi.org/10.1021/jp3101688.

Bahadir, E., Sezgintürk, M., 2015. Applications of electrochemical immunosensors for early clinical diagnostics. Talanta 132, 162–174. https://doi.org/10.1016/j.talanta.2014.08.063.

Baygu, Y., Gök, Y., 2018. A highly water-soluble zinc(II) phthalocyanines as potential for PDT studies: synthesis and characterization. Inorg. Chem. Commun. 96, 133–138. https://doi.org/10.1016/j.inoche.2018.08.004.

Bo, X., Zhou, M., Guo, L., 2017. Electrochemical sensors and biosensors based on less aggregated graphene. Biosens. Bioelectron. 89, 167–186. https://doi.org/10.1016/j.bios.2016.05.002.

Buber, E., Yuzer, A., Soylemez, S., Kesik, M., Ince, M., Toppare, L., 2017. Construction and amperometric biosensing performance of a novel platform containing carbon nanotubes-zinc phthalocyanine and a conducting polymer. Int. J. Biol. Macromol. 96, 61–69.

Calvo, E.J., Danilowicz, C., Diaz, L., 1993. Enzyme catalysis at hydrogel-modified electrodes with redox polymer mediator. J. Chem. Soc. Faraday. Trans. 89, 377–384. https://doi.org/10.1039/FT9938900377.

Chaiyo, S., Mehmeti, E., Siangproh, W., Hoang, T.L., Nguyen, H.P., Chailapakul, O., Kalcher, K., 2018. Non-enzymatic electrochemical detection of glucose with a disposable paper-based sensor using a cobalt phthalocyanine–ionic liquid–graphene composite. Biosens. Bioelectron. 102, 113–120. https://doi.org/10.1016/j.bios.2017.11.015.

Chirani, N., Yahia, L., Gritsch, L., Motta, F.L., Chirani, S., Faré, S., 2015. History and applications of hydrogels. J. Biomed. Sci. 04, 1–23. https://doi.org/10.4172/2254-609X.100013.

Claussen, J.C., Kumar, A., Jaroch, D.B., Khawaja, M.H., Hibbard, A.B., Porterfield, D.M., Fisher, T.S., 2012. Nanostructuring platinum nanoparticles on multilayered graphene petal nanosheets for electrochemical biosensing. Adv. Funct. Mater. 22, 3399–3405. https://doi.org/10.1002/adfm.201200551.

Costa de Oliveira, M.A., Mecheri, B., D'Epifanio, A., Placidi, E., Arciprete, F., Valentini, F., Perandini, A., Valentini, V., Licoccia, S., 2017. Graphene oxide nanoplatforms to enhance catalytic performance of iron phthalocyanine for oxygen reduction reaction in bioelectrochemical systems. J. Power Sources 356, 381–388. https://doi.org/10.1016/j.jpowsour.2017.02.009.

Crouch, E., Cowell, D.C., Hoskins, S., Pittson, R.W., Hart, J.P., 2005. Amperometric, screen-printed, glucose biosensor for analysis of human plasma samples using a biocomposite water-based carbon ink incorporating glucose oxidase. Anal. Biochem. 347, 17–23.

Cui, H.F., Zhang, K., Zhang, Y.F., Sun, Y.L., Wang, J., Zhang, W., De, Luong, J.H.T., 2013. Immobilization of glucose oxidase into a nanoporous TiO2 film layered on metallophthalocyanine modified vertically-aligned carbon nanotubes for efficient direct electron transfer. Biosens. Bioelectron. 46, 113–118.

Demirbaş, Ü., Kobak, R.Z.U., Barut, B., Bayrak, R., Koca, A., Kantekin, H., 2016. Synthesis and electrochemical characterization of tetra-(5-chloro-2-(2,4-dichlorophenoxy) phenol) substituted Ni(II), Fe(II) and Cu(II) metallophthalocyanines. Synth. Met. 215, 7–13.

Devasenathipathy, R., Karuppiah, C., Chen, S.-M., Palanisamy, S., Lou, B.-S., Ali, M.A., Al-Hemaid, F.M. a., 2015. A sensitive and selective enzyme-free amperometric glucose biosensor using a composite from multi-walled carbon nanotubes and cobalt phthalocyanine. RSC Adv. 5, 26762–26768.

Dhodapkar, R., Borde, P., Nandy, T., 2009. Super absorbent polymers in environmental remediation. Glob. NEST J. 11, 223–234.

Fogel, R., Mashazi, P., Nyokong, T., Limson, J., 2007. Critical assessment of the Quartz Crystal Microbalance with Dissipation as an analytical tool for biosensor development and fundamental studies: metallophthalocyanine-glucose oxidase biocomposite sensors. Biosens. Bioelectron. 23, 95–101. https://doi.org/10.1016/j.bios.2007.03.012.

Foster, C.W., Pillay, J., Metters, J.P., Banks, C.E., 2014. Cobalt phthalocyanine modified electrodes utilised in electroanalysis: nano-structured modified electrodes vs. Bulk modified screen-printed electrodes. Sensors 14, 21905–21922. https://doi.org/10.3390/s141121905.

Goenka, S., Sant, V., Sant, S., 2014. Graphene-based nanomaterials for drug delivery and tissue engineering. J. Control. Release 173, 75–88. https://doi.org/10.1016/j.jconrel.2013.10.017.

Gong, J., Li, D., Huang, J., Ding, L., Tong, Y., Li, K., Zhang, C., 2014. Synthesis of two novel water-soluble iron phthalocyanines and their application in fast chromogenic identification of phenolic pollutants. Catal. Lett. 144, 487–497. https://doi.org/10.1007/s10562-013-1178-0.

Gong, L., Young, R.J., Kinloch, I.A., Riaz, I., Jalil, R., Novoselov, K.S., 2012. Optimizing the reinforcement of polymer-based nanocomposites by graphene. ACS Nano 6, 2086–2095. https://doi.org/10.1021/nn203917d.

Gosselin, D., Gougis, M., Baque, M., Navarro, F.P., Belgacem, M.N., Chaussy, D., Bourdat, A.G., Mailley, P., Berthier, J., 2017. Screen-printed polyaniline-based electrodes for the real-time monitoring of loop-mediated isothermal amplification reactions. Anal. Chem. 89, 10124–10128. https://doi.org/10.1021/acs.analchem.7b02394.

Gregg, B.A., Heller, A., 1991. Redox polymer films containing enzymes. 2. Glucose oxidase containing enzyme electrodes. J. Phys. Chem. 95, 5976–5980. https://doi.org/10.1021/j100168a047.

Guadarrama-Fernández, L., Novell, M., Blondeau, P., Andrade, F.J., 2018. A disposable, simple, fast and low-cost paper-based biosensor and its application to the determination of glucose in commercial orange juices. Food Chem. 265, 64–69. https://doi.org/10.1016/j.foodchem.2018.05.082.

Hosseini, H., Mahyari, M., Bagheri, A., Shaabani, A., 2014. A novel bioelectrochemical sensing platform based on covalently attachment of cobalt phthalocyanine to graphene oxide. Biosens. Bioelectron. 52, 136–142. https://doi.org/10.1016/j.bios.2013.08.041.

Hou, S.F., Yang, K.S., Fang, H.Q., Chen, H.Y., 1998. Amperometric glucose enzyme electrode by immobilizing glucose oxidase in multilayers on self-assembled monolayers surface. Talanta 47, 561–567. https://doi.org/10.1016/S0039-9140(98)00081-2.

Iliev, V., Ileva, A., 1995. Oxidation and photooxidation of sulfur-containing compounds in the presence of immobilised phthalocyanine complexes. J. Mol. Catal. A Chem. 103, 147–153. https://doi.org/10.1016/S1381-1169(97)00101-5.

International Diabetes Federation, 2017. IDF Diabetes Atlas Eighth Edition 2017.

Jan, R., Habib, A., Khan, Z.M., Khan, M.B., Anas, M., Nasir, A., Nauman, S., 2017. Liquid exfoliated graphene smart layer for structural health monitoring of composites. J. Intell. Mater. Syst. Struct. 28, 1565–1574. https://doi.org/10.1177/1045389X16672729.

Kautzky-Willer, A., Harreiter, J., Pacini, G., 2016. Sex and gender differences in risk, pathophysiology and complications of type 2 diabetes mellitus. Endocr. Rev. 37, 278–316. https://doi.org/10.1210/er.2015-1137.

Komathi, S., Gopalan, A.I., Lee, K.P., 2009. Fabrication of a novel layer-by-layer film based glucose biosensor with compact arrangement of multi-components and glucose oxidase. Biosens. Bioelectron. 24, 3131–3134.

Kuznetsova, N.A., Gretsova, N.S., Derkacheva, V.M., Kaliya, O.L., Lukyanets, E.A., 2003. Sulfonated phthalocyanines: aggregation and singlet oxygen quantum yield in aqueous solutions. J. Porphyr. Phthalocyanines 07, 147–154. https://doi.org/10.1142/S1088424603000203.

Lawal, A.T., 2018. Progress in utilisation of graphene for electrochemical biosensors. Biosens. Bioelectron. 106, 149–178. https://doi.org/10.1016/j.bios.2018.01.030.

Layek, R.K., Nandi, A.K., 2013. A review on synthesis and properties of polymer functionalized graphene. Polymer 54, 5087–5103. https://doi.org/10.1016/j.polymer.2013.06.027.

Leznoff, C.C., Lever, A.B.P., 1996. Phthalocyanines: Properties and Applications. VCH publisher, New York. https://doi.org/10.1021/ja965771a.

Li, Z., Young, R.J., Wilson, N.R., Kinloch, I.A., Vallés, C., Li, Z., 2016. Effect of the orientation of graphene-based nanoplatelets upon the Young's modulus of nanocomposites. Compos. Sci. Technol. 123, 125–133. https://doi.org/10.1016/j.compscitech.2015.12.005.

Liu, J., Yang, Y., Hassanin, H., Jumbu, N., Deng, S., Zuo, Q., Jiang, K., 2016. Graphene-alumina nanocomposites with improved mechanical properties for biomedical applications. ACS Appl. Mater. Interfaces 8, 2607–2616. https://doi.org/10.1021/acsami.5b10424.

Lv, M., Liu, Y., Geng, J., Kou, X., Xin, Z., Yang, D., 2018. Engineering nanomaterials-based biosensors for food safety detection. Biosens. Bioelectron. 106, 122–128. https://doi.org/10.1016/j.bios.2018.01.049.

Malti, A., Edberg, J., Granberg, H., Khan, Z.U., Andreasen, J.W., Liu, X., Zhao, D., Zhang, H., Yao, Y., Brill, J.W., Engquist, I., Fahlman, M., Wågberg, L., Crispin, X., Berggren, M., 2016. An organic mixed ion-electron conductor for power electronics. Adv. Sci. 3, 1–9. https://doi.org/10.1002/advs.201500305.

Mani, V., Devasenathipathy, R., Chen, S.M., Gu, J.A., Huang, S.T., 2015. Synthesis and characterization of graphene-cobalt phthalocyanines and graphene-iron phthalocyanine composites and their enzymatic fuel cell application. Renew. Energy 74, 867–874.

Mani, V., Devasenathipathy, R., Chen, S.M., Huang, S.T., Vasantha, V.S., 2014. Immobilization of glucose oxidase on graphene and cobalt phthalocyanine composite and its application for the determination of glucose. Enzym. Microb. Technol. 66, 60–66.

Mashazi, P.N., Ozoemena, K.I., Nyokong, T., 2006. Tetracarboxylic acid cobalt phthalocyanine SAM on gold: potential applications as amperometric sensor for H2O2 and fabrication of glucose biosensor. Electrochim. Acta 52, 177–186.

Muckley, E.S., Jacobs, C.B., Vidal, K., Lavrik, N.V., Sumpter, B.G., Ivanov, I.N., 2017. Multi-mode humidity sensing with water-soluble copper phthalocyanine for increased sensitivity and dynamic range. Sci. Rep. 7, 1–11. https://doi.org/10.1038/s41598-017-10401-2.

Novoselov, K.S., Fal'Ko, V.I., Colombo, L., Gellert, P.R., Schwab, M.G., Kim, K., 2012. A roadmap for graphene. Nature 490, 192–200. https://doi.org/10.1038/nature11458.

Özcan, L., Şahin, Y., Türk, H., 2008. Non-enzymatic glucose biosensor based on over-oxidized polypyrrole nanofiber electrode modified with cobalt(II) phthalocyanine tetrasulfonate. Biosens. Bioelectron. 24, 512–517. https://doi.org/10.1016/j.bios.2008.05.004.

Ozoemena, K.I., Nyokong, T., 2006. Novel amperometric glucose biosensor based on an ether-linked cobalt(II) phthalocyanine-cobalt(II) tetraphenylporphyrin pentamer as a redox mediator. Electrochim. Acta 51, 5131–5136. https://doi.org/10.1016/j.electacta.2006.03.055.

Poitout, V., Hagman, D., Stein, R., Artner, I., Robertson, R.P., Harmon, J.S., 2006. Recent Advances in Nutritional Sciences Regulation of the Insulin Gene by Glucose and Fatty Acids. pp. 873–876 1.

Pu, Q., Li, J., Qiu, J., Yang, X., Li, Y., Yin, D., Zhang, X., Tao, Y., Sheng, S., Xie, G., 2017. Universal ratiometric electrochemical biosensing platform based on mesoporous platinum nanocomposite and nicking endonuclease assisted DNA walking strategy. Biosens. Bioelectron. 94, 719–727. https://doi.org/10.1016/j.bios.2017.03.062.

Schedin, F., Geim, A.K., Morozov, S.V., Hill, E.W., Blake, P., Katsnelson, M.I., Novoselov, K.S., 2007. Detection of individual gas molecules adsorbed on graphene. Nat. Mater. 6, 652–655. https://doi.org/10.1038/nmat1967.

Shahid, P., Ansari, Arfat, A., 2018. Conducting polymer hydrogels. Chem. Pap. https://doi.org/10.1007/s11696-016-0072-9. Elsevier Ltd.

Sode, K., Loew, N., Ohnishi, Y., Tsuruta, H., Mori, K., Kojima, K., Tsugawa, W., LaBelle, J.T., Klonoff, D.C., 2017. Novel fungal FAD glucose dehydrogenase derived from Aspergillus Niger for glucose enzyme sensor strips. Biosens. Bioelectron. 87, 305–311. https://doi.org/10.1016/j.bios.2016.08.053.

Ullah, S., Hamade, F., Bubniene, U., Engblom, J., Ramanavicius, A., Ramanaviciene, A., Ruzgas, T., 2018. In-vitro model for assessing glucose diffusion through skin. Biosens. Bioelectron. 110, 175–179. https://doi.org/10.1016/j.bios.2018.03.039.

Unnikrishnan, B., Palanisamy, S., Chen, S.-M., 2013. A simple electrochemical approach to fabricate a glucose biosensor based on graphene–glucose oxidase biocomposite. Biosens. Bioelectron. 39, 70–75.

Wang, H., Bu, Y., Dai, W., Li, K., Wang, H., Zuo, X., 2015. Well-dispersed cobalt phthalocyanine nanorods on graphene for the electrochemical detection of hydrogen peroxide and glucose sensing. Sensor. Actuator. B Chem. 216, 298–306.

WHO, 2016. Global report on diabetes. World Heal. Organ. https://doi.org/10.1128/AAC.03728-14.

Yang, W., Zhang, C.G., Qu, H.Y., Yang, H.H., Xu, J.G., 2004. Novel fluorescent silica nanoparticle probe for ultrasensitive immunoassays. Anal. Chim. Acta 503, 163–169. https://doi.org/10.1016/j.aca.2003.10.045.

Zagal, J., Bindra, P., Yeager, E., 1980. A mechanistic study of O2 reduction on water soluble phthalocyanines adsorbed on graphite electrodes. J. Electrochem. Soc. 127, 1506–1517.

Zhang, Y.Q., Fan, Y.J., Cheng, L., Fan, L.L., Wang, Z.Y., Zhong, J.P., Wu, L.N., Shen, X.C., Shi, Z.J., 2013. A novel glucose biosensor based on the immobilization of glucose oxidase on layer-by-layer assembly film of copper phthalocyanine functionalized graphene. Electrochim. Acta 104, 178–184.

Zhu, Y., Murali, S., Cai, W., Li, X., Suk, J.W., Potts, J.R., Ruoff, R.S., 2010. Graphene and graphene oxide: synthesis, properties, and applications. Adv. Mater. 22, 3906–3924. https://doi.org/10.1002/adma.201001068.